*Asian Journal of Chemical Sciences*

***Volume 14, Issue 3, Page 27-39, 2024; Article no.AJOCS.114762***
***ISSN: 2456-7795***

# Preparation and Characterization of Ferrihydrite: Application in Arsenic Removal from Aqueous Solutions

**Rasmane Tiendrebéogo [a,b], Yacouba Sanou [a*], Samuel Paré [a] and Aboubacar Senou [b]**

*[a] Laboratory of Analytical, Environmental and Bio-Organic Chemistry, University Joseph KI ZERBO, 03 BP 7021 Ouagadougou 03, Burkina Faso.*
*[b] Laboratory of Mineral, Water and Environment Analysis, SENEXEL BP312 Ouagadougou Kossyam, Burkina Faso.*

***Authors' contributions***

*This work was carried out in collaboration among all authors. All authors read and approved the final manuscript.*

***Article Information***

DOI: https://doi.org/10.9734/ajocs/2024/v14i3307

**Open Peer Review History:**
This journal follows the Advanced Open Peer Review policy. Identity of the Reviewers, Editor(s) and additional Reviewers, peer review comments, different versions of the manuscript, comments of the editors, etc are available here: https://www.sdiarticle5.com/review-history/114762

***Original Research Article***

***Received: 04/03/2024***
***Accepted: 08/05/2024***
***Published: 18/05/2024***

## ABSTRACT

Arsenic pollution is a public health hazard in Burkina Faso due to its impact on human health and water resources. To mitigate this pollution, ferrihydrite material has been synthesized and characterized to be used as adsorbent for arsenic removal in aqueous solutions. This study aimed to contribute to improve of access to clean drinking water by removing arsenic from water using ferrihydrite. Arsenic species such as As(III) and As(V) were removed through batch adsorption. Experiments were carried out in batch mode using arsenic aqueous solutions. The characterization of ferrihydrite using Scanning Electron Microscopy (SEM) coupled with Energy Dispersive Spectroscopy (EDX), X-ray Diffraction (XRD), Infrared (IR), and Brunauer Emmett Teller (BET) showed that an amorphous and microporous 2-line ferrihydrite. The total specific surface area and pH at point of zero charge ($pH_{pzc}$) were 184.518 $m^2/g$ and 9.41, respectively. The optimal adsorbent

**Corresponding author: E-mail: prosperyacson@gmail.com;*

***Cite as:*** *Tiendrebéogo, R., Sanou, Y., Paré, S., & Senou, A. (2024). Preparation and Characterization of Ferrihydrite: Application in Arsenic Removal from Aqueous Solutions. Asian Journal of Chemical Sciences, 14(3), 27–39. https://doi.org/10.9734/ajocs/2024/v14i3307*

doses were 4 g/L for As (V) and 8 g/L for As (III). The optimum pH range for the adsorption of As (V) and As (III) was between 2 and 10, The maximum adsorption capacity was 15.07 mg/g for As(V) and 13.01 mg/g for As(III) with increasing concentration between 2 and 16 mg/L. Equilibrium time for As (V) and As (III) on ferrihydrite was found to be 720 min and 960 min, respectively. The adsorption of As(V) and As(III) was consistent with the Langmuir monolayer model on ferrihydrite. Arsenic adsorption was occurred according to spontaneous chemical reaction. Arsenic removal was occurred on a monolayer following the pseudo-second order kinetic.

*Keywords: Adsorption; arsenic; characterization; ferrihydrite; removal.*

## 1. INTRODUCTION

In different forms, arsenic compounds are known for their high toxicity to living organisms, mainly humans and animals [1,2]. Due to human activities, the increase in global mining and mineral processing processes contributed to the accumulation of arsenic in waste rock and mine drainage water [2,3,4]. The transfer of arsenic with other heavy metals in soil and water resources has been observed in many regions of the world [5,6,7]. Arsenic (III) is less common in water and more toxic than arsenic (V) in different forms [2,5]. In addition to its role as a trace element in life, arsenic exposure through daily consumption of arsenic water is responsible for many diseases (cancers, respiratory problems, etc.) worldwide [8,9,10]. In Burkina Faso, arsenic contamination has been noted in several regions due to the consumption of water with concentrations higher than the standard of 10 µg/L according to the World Health Organization (WHO) [10,11]. Boreholes and water sources built in rural areas by the state and partners have been closed for contamination reasons linked to arsenic [10,11]. Arsenic removal from water at a rate of less than 10 µg/L (WHO standard) is becoming a global necessity for the supply of drinking water in developing countries [2,9]. To reduce the harmful effects of arsenic compounds, treatment techniques such as filtration, coagulation-precipitation, reverse osmosis, electrodialysis, adsorption, and coupled techniques have been developed [12,13,14]. Among these techniques, adsorption has been studied in recent years owing to its effectiveness, economy, low cost, and environmental friendliness [14,15]. In the implementation of adsorption technique, the adsorbent material must be effective, selective, and have a high specific surface area to accumulate different forms of arsenic [15,16]. Adsorbents such as activated carbon, clays, laterites, and metal oxy-hydroxides have been tested for the removal of As (III) and As (V) in water [15,16,17]. Literature indicated that adsorbents based on iron oxides and hydroxides are effective for the adsorption of different forms of arsenic because of their amphoteric character [18,19,20].

In this work, ferrihydrite has been used as adsorbent for arsenic removal. Specifically, ferrihydrite has been prepared and characterized using analytical methods. The mechanisms and kinetics of As (III) and As (V) removal using ferrihydrite were evaluated in batch mode under the various operating parameters.

## 2. MATERIALS AND METHODS

### 2.1 Preparation of Ferrihydrite

To prepare the ferrihydrite, the method described by Scwertmann et al*.* [21] was used. Indeed, 100 mL of a 0.25 M ferric nitrate monohydrate solution (purity ≥ 98%) (Sigma-Aldrich) was prepared with distilled water at initial pH of 2.08. The ferrihydrite was stored in an enclosure at a temperature between 19 and 21°C for future use in water treatment.

### 2.2 Physico-chemical Characterization of Ferrihydrite

#### 2.2.1 Physical characterization

The moisture content (TH) of the ferrihydrite was determined after centrifugation of the paste to evaluate the quantity of free water that it contained before drying. 50 g of ferrihydrite ($m_1$) was placed in an oven at 110°C for 72 h until a constant mass $m_2$ was obtained. The moisture content (TH) of the ferrihydrite has been calculated according to the following relationship [19]:

$$\mathrm{TH}\ (\%) = \left(\frac{m_1 - m_2}{m_1}\right) \times 100 \qquad (1)$$

The bulk density (d) of the ferrihydrite was determined using a method described elsewhere

[16]. Equation 2 was used to determine the bulk density of ferrihydrite:

$$d = \frac{(m_1 - m_0)}{V} \quad (2)$$

The pH at the point of zero charge ($pH_{PZC}$) has been studied to understand the neutral surface charge of ferrihydrite [22]. The $pH_{PZC}$ value was determined from the curve ΔpH =pHi - pHf as a function of initial pH and this curve intercepts the abscise where of ΔpH = 0 [23].

The surface area and the pore dimensions of the ferrihydrite were analyzed using Micromeritic (TriStar II plus version 3.02) controlled with MicroActive software. Before nitrogen (N2) adsorption at 77.350 K, the ferrihydrite was dried and dispersed in a glass quantrachrome cell at 105 °C for 24 h to remove the adsorbed water and gas. The surface area was determined using the Brunauer, Emmett, and Teller (BET) method and the one of Langmuir [22, 24]. The nitrogen adsorption and desorption isotherms obtained by Barrett, Joyner, and Halenda (BJH) method were used to determine the volume of pores.

### 2.2.2 Chemical characterization

Elemental chemical analysis of the ferrihydrite was carried out using a Microwave Plasma Atomic Emission Spectrometer (MP-AES, Agilent 4200) controlled by the Spectra software. The powder of ferrihydrite was mineralized by the «eau regale method» according to the following protocol. Indeed, 10 g of the dry powder was weighed into a 100 mL gauge flask. Subsequently, 15 mL of hydrochloric acid (37%, Honeywell) and 5 mL of nitric acid (68%, Flucka) of analytical grade (AR) were added and heated to a temperature of 200±5 °C on a hot plate for one hour (1 h). After cooling, the flask was completed up to the gauge mark, homogenized, and used for the determination of chemical elements by MP-AES previously calibrated with standard solution [24].

The Fourier Transform - infrared (FT-IR) spectrum was recorded in the range of 500 to 4000 $cm^{-1}$ with a resolution of 4 $cm^{-1}$ using an OUAFO device (controlled by OPUS software) to evaluate the surface chemical functions.

The mineral phase of the ferrihydrite was studied using a Shimadzu diffractometer equipped with a copper tube and graphite monochromator. The diffractogram was collected in an angular range of 2Θ from 2° to 90° at a speed of 2° $min^{-1}$ under a voltage of 40 kV and intensity of 30 mA [23].

Scanning Electron Microscopy (SEM) was used to study the morphology and surface composition of the ferrihydrite using a Microspec-WDX 600/OXFORD coupled to energy dispersive spectroscopy (EDX) [19, 25].

## 2.3 Preparation of Arsenic Solutions

A stock solution of As (III) (1000 ppm) was prepared by dissolving a sodium arsenite salt ($NaAsO_2$) in a solution of 20% NaOH (Flucka) [20]. The As (V) solutions of were prepared from a stock solution of 1000 ppm ($Na_2HAsO_4{\cdot}7H_2O$, Merck) by dilution with ultrapure distilled water. Reagents such as NaOH (Flucka) and $HNO_3$ (Sigma-Aldrich) were of analytical grade (AR) and were used to adjust the pH of the matrix solutions. The pH of As (III) and As (V) solutions was ranged between 7 and 8, and controlled with a branded portable pH meter (HANNA, waterproof HI98318). pH of the solutions was adjusted using 0.1 M NaOH and 0.1 M $HNO_3$ solutions.

## 2.4 Arsenic Removal Experiments

Batch experiments were conducted to remove As (III) and As (V) from aqueous solutions. To assess the effects of operating parameters on adsorption process, 25 mL solution of As (III) or As (V) at a concentration of 5 mg/L was added to 1.0 g of ferrihydrite in test tubes and initial pH was adjusted between 2 and 12. Absorbent dose was varied over a range of 4 g/L to 14 g/L using initial arsenic concentration of 5 mg/L. The effect of initial arsenic concentration was then evaluated using concentration ranging from 1 to 16 mg/L. Similar experiments were carried out to assess adsorption kinetics by testing from 01 h to 24 h with a 10g/L dose of adsorbent at an arsenic concentration of 5 mg/L. All experiments were running for 24 h at room temperature in the laboratory 24 ± 0.15°C.

Residual arsenic concentration has been analyzed with a Microwave Plasma Atomic Emission Spectrometer (MP-AES Agilent 4200) after filtration. The evaluation of the adsorption efficiency using ferrihydrite was carried out using the percentage of removal denoted As (%) and the adsorption capacity denoted Qe (mg/g). The arsenic removal was calculated using the following relation:

$$\text{As}\ (\%) = \frac{C_i - C_e}{C_i} \times 100 \quad (3)$$

The adsorption capacity of ferrihydrite was determined by the following formula:

$$Q_e(\text{mg/g}) = \frac{(C_i - C_e) \times V}{m} \quad (4)$$

Where Ci and Ce (mg/L) represent the initial and equilibrium concentrations of As (III) or As (V), respectively, m (g) and V (L) are the mass of the ferrihydrite and the volume of solution, respectively.

## 3. RESULTS AND DISCUSSION

### 3.1 Characteristics of Ferrihydrite

Fig. 1 shows a moist red-brown chocolate cake batter (Fig. 1A) and brown-colored ferrihydrite powder (Fig. 1B). The mesh size of the ferrihydrite grains used in this work is less than or equal to 75 µm. The appearance and texture of the ferrihydrite powder obtained were similar to those reported by Otgon *et al.* [18] at pH (3-4).

Physicochemical characteristics of the ferrihydrite are listed in Table 1. In this Table, we noticed that ferrihydrite has a large positive surface area relative to its basic pH at point of zero charge ($pH_{PZC}$). In addition, this material contained a very high moisture content (69%). Ferrihydrite's positively charged surface is therefore capable of adsorbing anions such as arsenic species [23]. The bulk density, which is almost half the density of pure iron (d = 7.874 g/cm$^3$), indicates the predominance of iron in the ferrihydrite [19]. The specific surface area of the ferrihydrite powder (184.518 m$^2$/g) is lower than the value reported by Milton et al. [26]. The higher Langmuir surface area than the other surfaces recorded in Table 1 indicates that monolayer adsorption may control the removal of As (V) or As (III) from ferrihydrite [15,19]. The quantitative analysis of ferrihydrite showed the high content of iron (1257 mg/L) confirming its nature of iron oxyhydroxide.

Spot chemical analysis of the surface using EDX (Fig. 2) revealed that the ferrihydrite was mainly composed of iron (49.54%) and oxygen (34.18%). Other chemical elements were present in the ferrihydrite such as carbon (11.08%), sodium (2.50%), titanium (1.53%) and aluminum (1.05%). Qualitative analysis of the ferrihydrite corroborated by the results of the quantitative analysis (Table 1).

The IR spectrum in Fig. 3 shows the characteristic bands of the ferrihydrite. The different vibration bands were assigned according to the literature [19,26,27]. The bands around 3400 cm$^{-1}$ correspond to the stretching vibrations of the O-H bonds in the surface hydroxyl groups and water molecules. The wave numbers around 1630, 1400, and 900 cm$^{-1}$ would correspond to adsorbed water molecules, deformation of Fe-O bonds, and deformation of Fe-OH, respectively. Milton et al. [26] showed that the characteristic bands of ferrihydrite are mainly due to the hydroxyl O-H groups, the Fe-O and Fe-OH function of the structure. The relatively weak intensity of the stretching bands of the O-H bonds in the hydroxyl groups can be explained by the metastable nature of ferrihydrite [28].

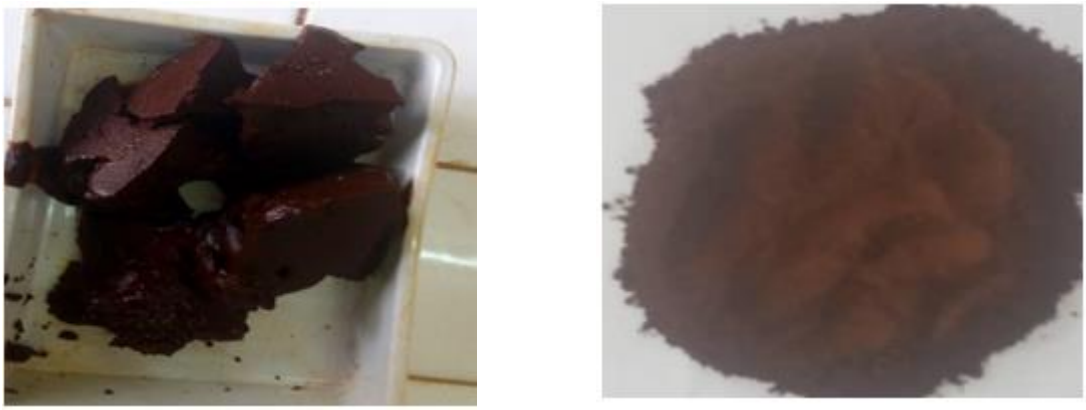

**A: Moist ferrihydrite** **B: Ferrihydrite powder at 75 µm**

**Fig. 1. Images of the prepared ferrihydrite**

**Table 1. Physicochemical characteristics of ferrihydrite powder**

| Physical parameter | Quantitative value |
|---|---|
| Particle size (µm) | ≤ 75 |
| Moisture content TH (%) | 69.00 |
| Bulk density (d) | 4.07 |
| pH at the point of zero charge ($pH_{PZC}$) | 9.41 |
| BET specific surface area ($m^2/g$) | 59.986 |
| Langmuir specific surface area ($m^2/g$) | 73.315 |
| External specific surface area ($m^2/g$) | 51.216 |
| Total specific surface area (SS) ($m^2/g$) | 184.518 |
| Total pore volume ($cm^3/g$) | 0.052 |
| **Quantitative analysis of ferrihydrite** | |
| Fe (mg/L) | 1257.010 |
| Al (mg/L) | * |
| Cu (mg/L) | * |
| Pb (mg/L) | * |
| Si (mg/L) | * |
| Ti (mg/L) | 0.019 |
| Na (mg/L) | 2.310 |
| Zn (mg/L) | 0.007 |

**Not determined*

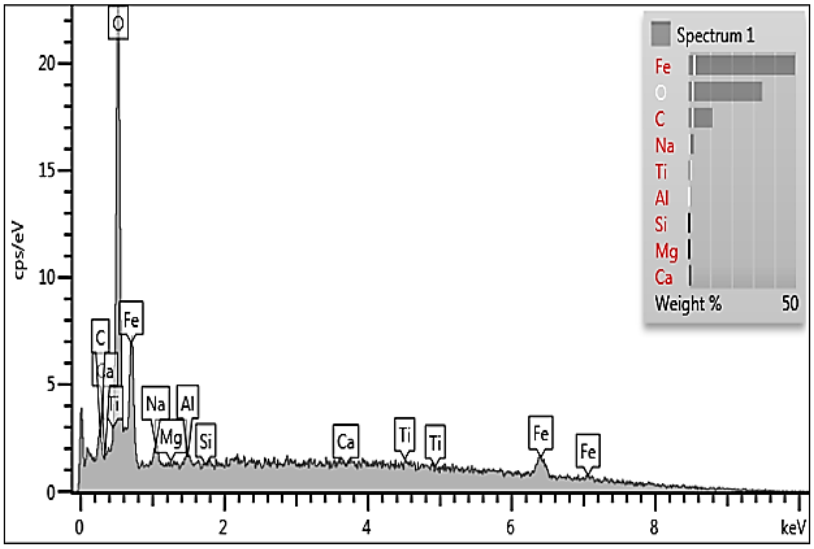


**Fig. 2. Spectrum EDX**

The X-Ray diffraction (XRD) pattern of the ferrihydrite is shown in Fig. 4. It highlighted the presence of two broad lines at 2θ values close to 35° and 67°. According to the literature [18,28], this diffraction pattern can be attributed to "2-line" ferrihydrite rather than "6-line" ferrihydrite, whose diffraction pattern shows 6 lines. Background noise with relatively low peak intensities is observed in the diffraction pattern, indicating that the synthesized ferrihydrite is amorphous format. Otgon et al. [18] showed that the intensity of the peaks depended on the morphology and crystallinity of ferrihydrite. The ferrihydrite prepared could therefore be an amorphous 2-line ferrihydrite.

The images in Fig. 5 show the surface morphology of ferrihydrite powder particles at different magnification scales. Magnification A (5X) shows a cluster of aggregates formed by small particles. Whereas magnification C (100 X) shows whitish irregular spherical shapes with relatively close pores indicating a larger specific surface area with small pore volumes [21,26].

These irregularly distributed whitish particles indicate the very amorphous character of the ferrihydrite powder revealed by the diffractogram. In their studies on the removal of As (V) by iron-doped activated carbon, Sanou [19] showed that the whitish particles were due to the presence of iron and its magnetic nature. The particle clusters in the SEM images could be conglomerates of micron-sized nanoparticles visible under transmission electron microscopy (TEM) [29,30].

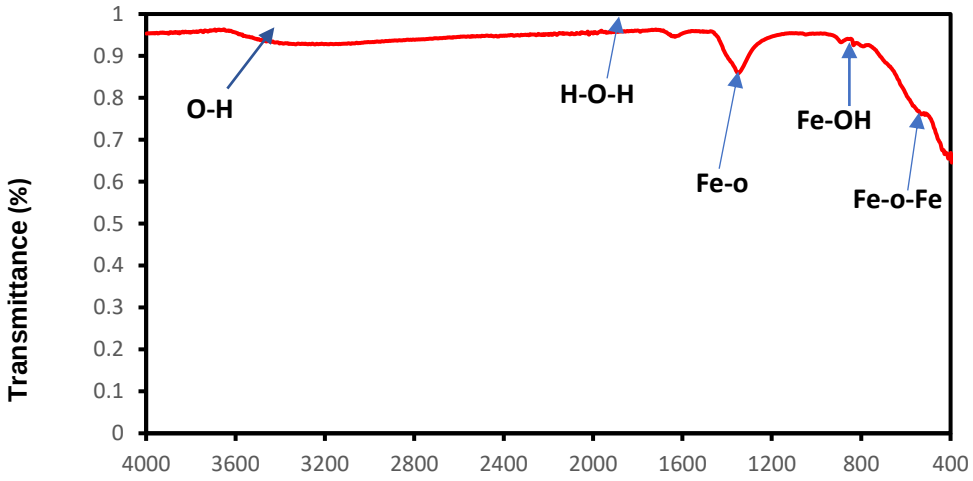


**Fig. 3. FT - IR spectrum of ferrihydrite powder**

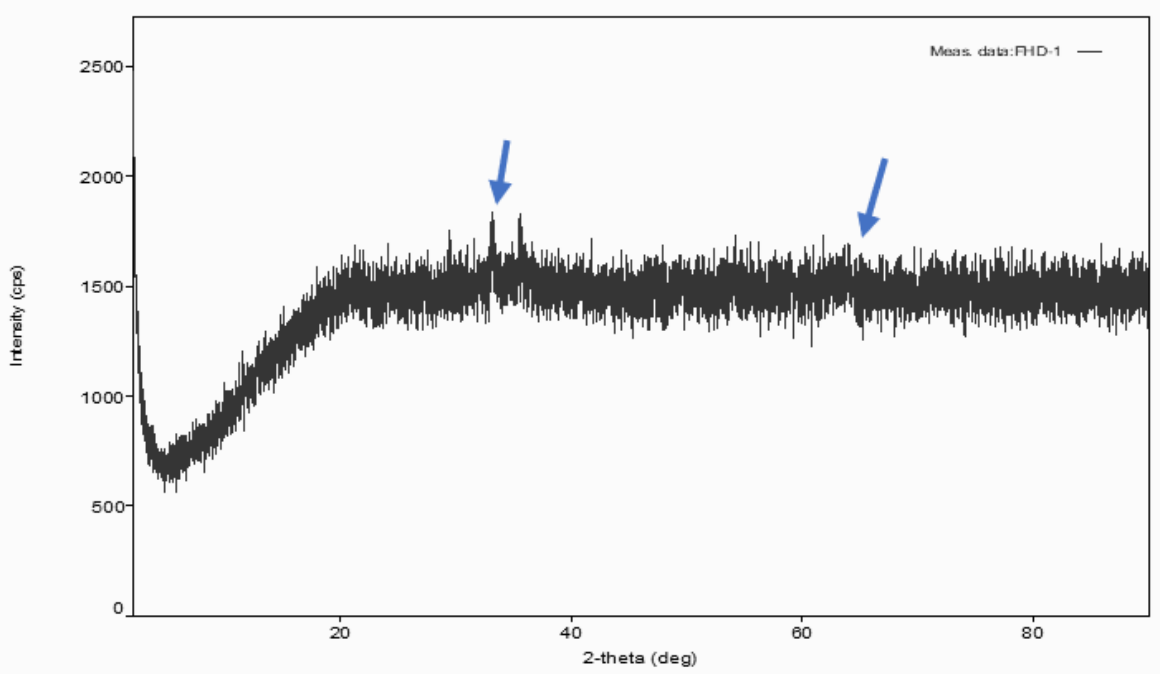


**Fig. 4. XRD pattern of ferrihydrit**

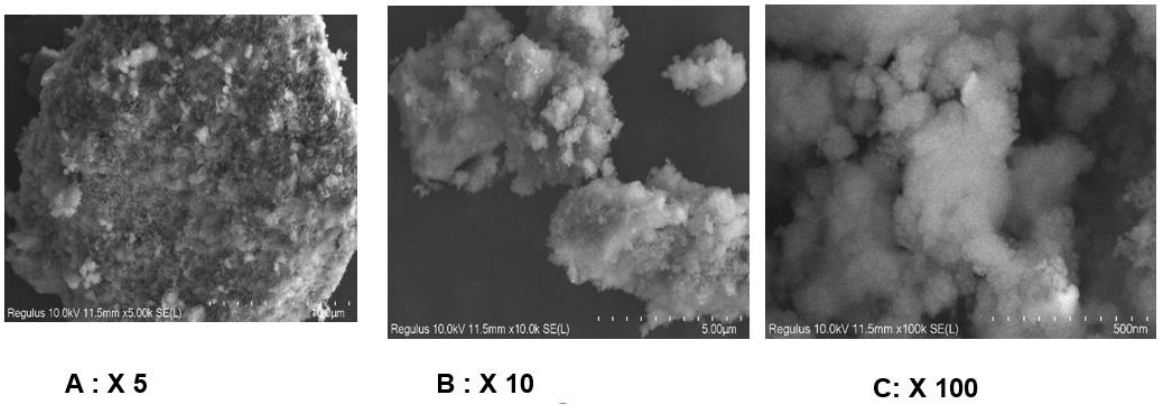


**Fig. 5. SEM images of ferrihydrite at 5X, 10X, 100X magnification at 10 KV**

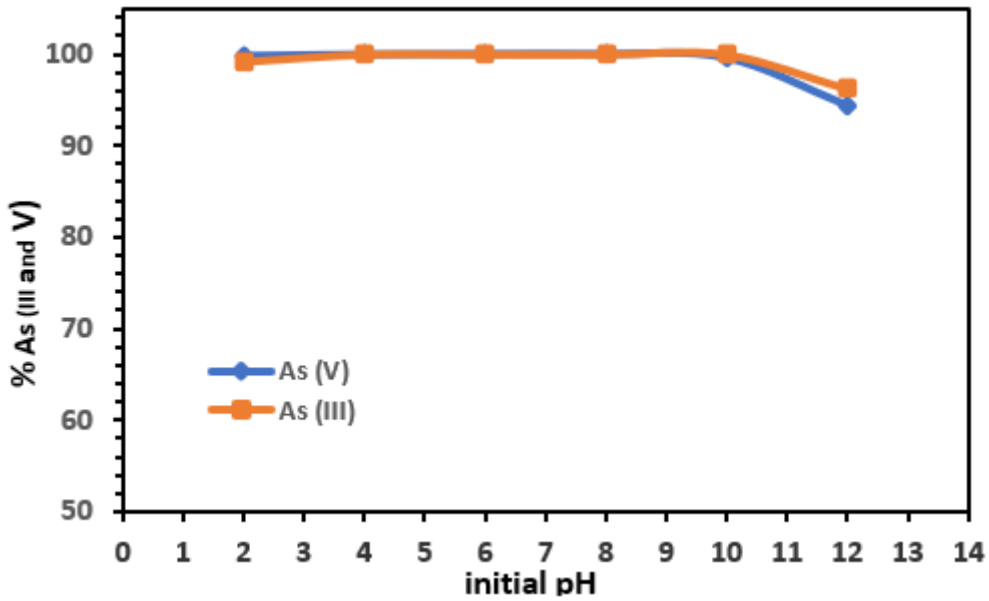


**Fig. 6. Effect of initial pH on the removal of As (V) and As (III) with $C_0$ = 5mg/L, m = 1.0 g, and t = 24h**

## 3.2 Influence of Operating Parameters on Arsenic Removal

### 3.2.1 Effect of initial pH

Fig. 6 shows the behavior of adsorption of As (III) and As (V) over the pH range of 2–12. Experimental results revealed that As (III) and As (V) were totally removed (100%) until pH ZPC = 9.41.

The removal rate decreased slightly in the pH range 10–12 for As (III) and As (V). The efficiency of the adsorption of different forms of arsenic, such as $H_3AsO_4$, $H_2AsO_4$-, $HAsO_4^{2-}$ and $H_3AsO_3$ at a pH lower than 9.41 could be explained by a process of attraction due to the positive charge of the ferrihydrite surface. However, beyond $pH_{PZC}$ = 9.41, the decrease in arsenic removal could be explained by the repulsion of the ionic forms of arsenic ($H_3AsO_3$, $H_2AsO_3^-$, $AsO_3^{3-}$, $AsO_4^{3-}$) by the negatively charged surface [23,24]. The adsorption of neutral forms ($H_3AsO_4$ and $H_3AsO_3$) in the pH range ≤ $pH_{PZC}$ would be an ionization of the arsenate and arsenite forms on ferrihydrite followed by a ligand exchange mechanism [23]. The average equilibrium pH of the final pH value was 7.29. Thus, the mechanism for the removal of arsenic species on the ferrihydrite surface would be bidentate or monodentate [18,27]. The optimal pH range is 2–10, which would

correspond to the range indicated by Qi et al. [31].

### 3.2.2 Effect of adsorbent amount

The influence of the mass of ferrihydrite was evaluated for adsorbent doses ranging from 4 to 40 g/L with an initial concentration of 5 mg/L of As (V) and As (III) at pH 7.45 for 24 h. Results (Fig. 7) showed an increase in the arsenic removal from 99.64 to 100% for As (V), and from 87 to 100% for As (III). The optimal adsorbent doses under these conditions were 4 g/L for As (V) and 8 g/L for As (III) on the ferrihydrite. The adsorbent dose for As (III) was double that for As (V) because of the oxidation of As (III) to As (V) before its fixation on the surface of ferrihydrite [25,31]. The increase in the removal rate was due to the increase in the number of active sites on ferrihydrite. The adsorption capacity of ferrihydrite depends on the number of active sites and specific surface area [31].

### 3.2.3 Effect of initial arsenic concentration

The behavior of the adsorption of As (V) and As (III) onto ferrihydrite was studied over a concentration range of 2–16 mg/L at pH (6.89) with a mass of 1.0 g during 24 h. Fig. 8 revealed that the removal percentages of As (V) and As (III) on the ferrihydrite surface decreased with the increase of initial arsenic concentration. For As (V), the removal percentage decreased from 100 to 93.95% while by removing As (III), it decreased from 100 to 85.10%. The adsorption capacity of ferrihydrite increased from 2.0 to 15.07 mg/g for As (V) and from 2.0 to 13.01 mg/g for As (III). This increase in adsorption capacity could be explained by the increase in initial As (V) and As (III) ions fixed on the active sites of the ferrihydrite [20,32]. However, the decrease in arsenic removal percentage could be due to the limited number of arsenic ions adsorbed on the ferrihydrite at low arsenic concentrations [32,33]. The optimal concentration of ferrihydrite was 5 mg/L for As (V) and 10 mg/L for As (III).

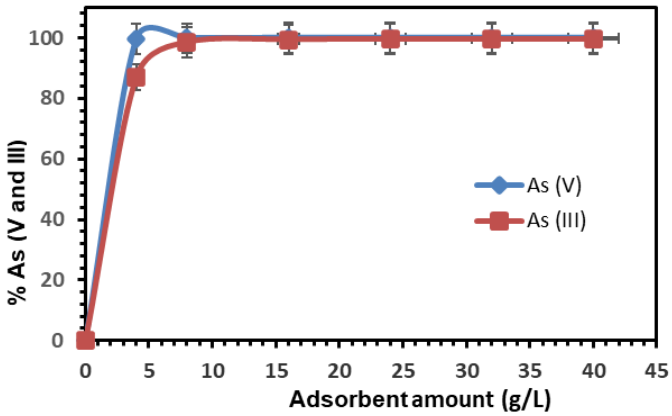


**Fig. 7. Effect of the adsorbent dose with $C_0$ = 5 mg/L, pH = 7.68 and t = 24 h**

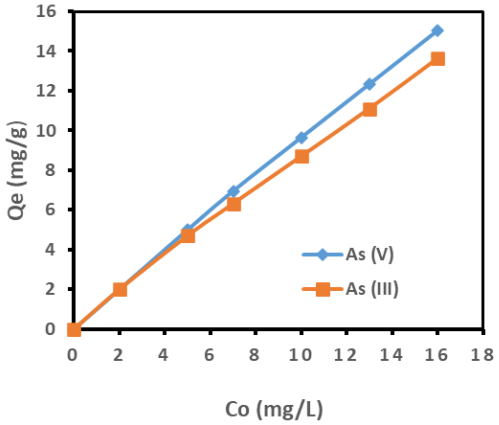


**Fig. 8. Effect of initial arsenic concentration with m=1.0 g, pH = 6.89 and t= 24h**

### 3.2.4 Effect of contact time

The effect of the contact time was studied from 1h to 24 h (60-1440 min) with a concentration of 5 mg/L and a mass of 1.0 g as shown in Fig. 9. The removal percentage as a function of the contact time showed an increase according two steps:

First step indicated an increase of arsenic (V) removal from 78 to 99.80% when the contact time was increased between 60 and 720 min. Thus, the removal of As (III), increased from 70 to 99.00% with an increase of contact time between 60 and 960 min. The second step indicated that arsenic removal remained constant after 720 min and 960 min for As(V) and As (III), respectively.

The equilibrium time for optimum removal of As (V) and As (III) on ferrihydrite was 720 min (12h) and 960 min (16h) corresponding to adsorption capacity of 623.75 and 618.75 µg/g respectively for As(V) and As (III). Adsorption of As (V) and As (III) onto ferrihydrite could be chemical reactions of the internal and external complexes on the functional groups of the adsorbent, as shown by the IR spectrum [20,27].

### 3.2.5 Modelling of isotherms

The adsorption behavior of As (V) and As (III) on ferrihydrite as a function of the initial concentration was modeled using the Langmuir and Freundlich equilibrium isotherms [15,33,34]. Langmuir isotherm model describes the monolayer adsorption with homogenous sites of adsorbent, while multilayer adsorption and heterogenous sites were described by Freundlich isotherm model.

The linearized form of the Langmuir isotherm model is given by the relation:

$$\frac{C_e}{Q_e} = \frac{1}{Q_m}(C_e) + \frac{1}{K_L Q_m} \quad (5)$$

The equation of the Freundlich model is given by the following relation:

$$LnQ_e = lnK_f + \frac{1}{n} lnC_e \quad (6)$$

Fig. 9 shows the plots Ce/Qe = f(Ce) and LnCe = f(Ce) as functions of the equilibrium concentration Ce for the Langmuir and Freundlich models. The slopes and intercept of the curves were used to calculate the different constants listed in Table 2.

The values of correlation coefficient $R^2$ with the Langmuir and Freundlich isotherms indicate a good correlation with the experimental data. Using Langmuir isotherm, the adsorption capacity values for As (V) and As (III) were 12.01 and 11.36 mg/g, higher than the values of $K_f$ obtained with the Freundlich model (Table 2). Values of Qm with Langmuir model are close to experimental values of $Q_{exp}$ (13.01 and 15.07 mg/g for As (III) and As (V), respectively). Consequently, the removal of As (V) and As (III) have been occurred through the monolayer adsorption with homogeneous active sites. The Freundlich affinity constants (n) of As (V) and As (III) are 2.78 and 3.86 respectively, and are all greater than 1, indicating favourable adsorptions [19,35].

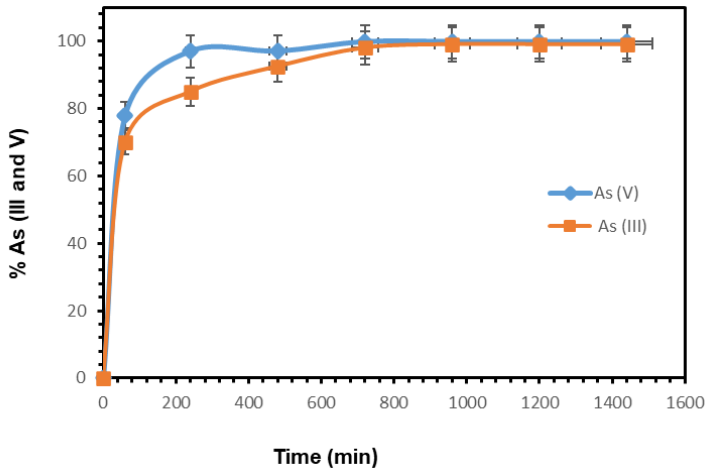


**Fig. 9. Effect of initial time on the removal of As (V) and As (III) with $C_0$ = 5 mg/L, m= 1.0 g and pH = 7.21**

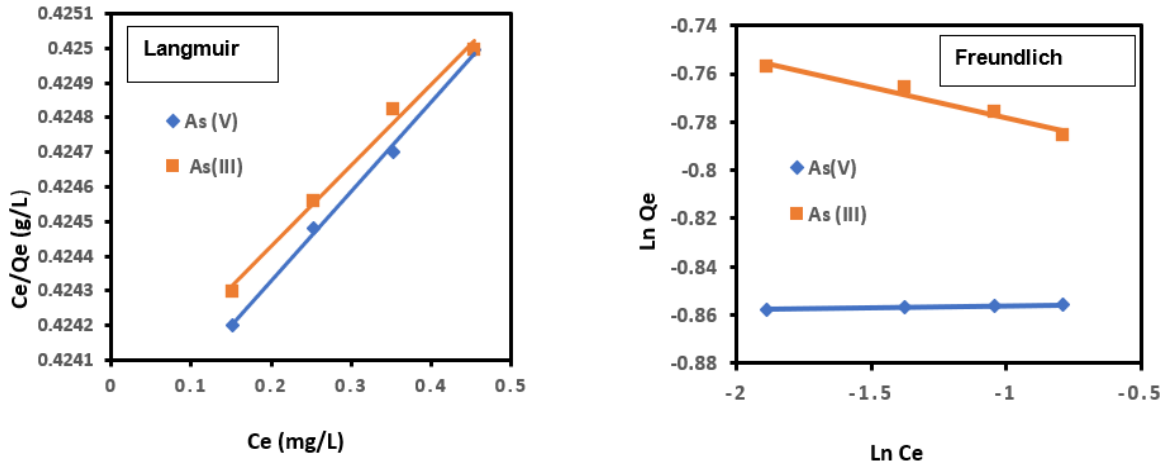


**Fig. 10. Representation of Langmuir and Freundlich isotherms for As (V) and As (III)**

**Table 2. Langmuir and Freundlich constants**

| Ferrihydrite | Langmuir | | | Freundlich | | | |
|---|---|---|---|---|---|---|---|
| | $Q_m$ (mg/g) | $K_L$ (L/mg) | $R^2$ | $K_f$ (mg/g) | n | $R^2$ | Qexp (mg/g) |
| **As (V)** | 12.01 | 1.73 | 0.98 | 10.31 | 2.78 | 0.97 | 15.07 |
| **As (III)** | 11.36 | 3.28 | 0.99 | 10.96 | 3.86 | 0.98 | 13.01 |

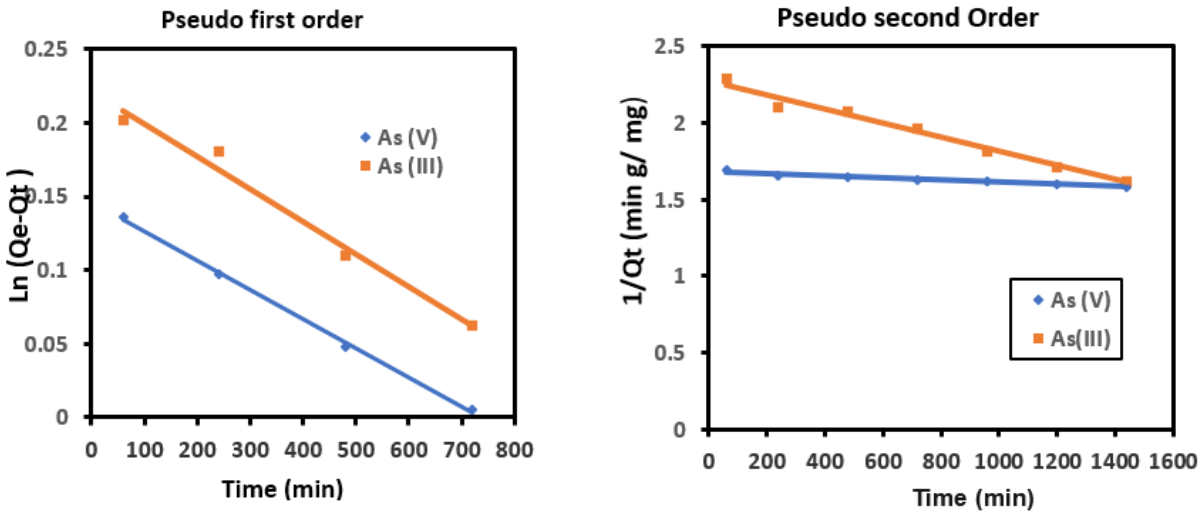


**Fig. 11. Representation of the kinetic models for the removal of As (V) and As (III) on ferrihydrite**

**Table 3. Kinetic constants in the removal of As (V) and As (III) on ferrihydrite**

| Ferrihydrite | Pseudo-first-order | | | | Pseudo-second-order | | | |
|---|---|---|---|---|---|---|---|---|
| | $Qe_{exp}$ | $Qe_{theo}$ | $K_1$ | $R^2$ | $Qe_{exp}$ | $Qe_{theo}$ | $K_2$ | $R^2$ |
| | mg/g | mg/g | $min^{-1}$ | | mg/g | mg/g | $min^{-1}$ | |
| As (V) | 5.35 | 1.55 | 0.012 | 0.99 | 5.35 | 5.29 | 3.14 | 0.98 |
| As (III) | 4.95 | 1.45 | 0.010 | 0.98 | 4.95 | 5.18 | 3.78 | 0.97 |

The equilibrium parameter $R_L$ and the Gibbs free energy ($\Delta G$) have been evaluated from the following relations:

$$\Delta G_0 = - RT. Ln K_L \quad (7)$$

$$R_L = \frac{1}{1+K_L C_O} \quad (8)$$

The calculated $R_L$ values were between 0 and 1, indicating a favorable adsorption process for As (V) and As (III). The negative Gibbs free energies are 2.70 and 1.24 kJ/mole respectively for As (V) and As (III) indicated that the reactions on ferrihydrite are not spontaneous [19].

### 3.2.6 Kinetic modeling

To study the kinetic of arsenic removal, the pseudo-first-order and pseudo-second-order model described by Lagergren and the one given by Ho and Mckay, respectively have been widely studied [19, 35]. The integration of the Lagergren's equation (9) and the one of Ho and McKay (10) are given in the following formulas:

$$Ln (Q_e - Q_t) = ln Qe - k_1 t \quad (9)$$

$$\frac{t}{Q_t} = \frac{1}{Q_e} t + \frac{1}{K_2 Qe^2} \quad (10)$$

The representations of these equations were given in Fig. 10.

The correlation coefficients ($R^2$) ranged from 0.97 to 0.99 for both models indicate that data are perfectly correlated between the variables. Using the pseudo-second kinetic model, the theoretical values of the adsorption capacity (Qe theo) are close to the experimental values (Qe exp) indicating that arsenic removal followed the pseudo-second-order model. The removal rate constants $K_2$ (Table 3) of As (III) was greater than that of As (V), indicating faster removal of As (III) on ferrihydrite. Consequently, chemisorption would control the adsorption process of As (V) and As (III) on the surface of ferrihydrite through an inner-sphere reaction [19,35].

## 4. CONCLUSION

This study enabled the successful preparation and characterization of ferrihydrite as adsorbent in arsenic removal. Characterization of the powder ferrihydrite indicated an amorphous 2-line ferrihydrite with hydroxide and surface hydroxyl functionalities to give butter results. The efficiency of ferrihydrite in arsenic removal, mainly As (V) or As (III) species depended on the initial pH, adsorbent dose, initial concentration, and contact time. The mechanism of the removal of arsenic on ferrihydrite could be described by monolayer adsorption occurred following a not spontaneous process. The removal of As (III) or As (V) has been occurred according the pseudo-second-order kinetic and chemisorption process.

## ACKNOWLEDGEMENTS

Authors would like to thank the SENEXEL laboratory for the support in MP-AES tests and analyses.

## COMPETING INTERESTS

Authors have declared that no competing interests exist.

## REFERENCES

1. Sayan B, Avishek T, Shubhalakshmi S, Tuyelee D, Abhijit D, Kaushik G, Nalok D. Arsenic contaminated water remediation: A state-of-the-art review in synchrony with sustainable development goals. Groundwater for Sustainable Development. 2023;23:2352-801X. Available:https://doi.org/10.1016/j.gsd.2023.101000
2. Hifza R, Rebecca S, Paul K. Human health risk assessment for arsenic: A critical review. Critical Reviews in Environmental Science and Technology; 2016. DOI: 10.1080/10643389.2016.1245551
3. Ackmez M, Sanjay KS, Vinod KG, Chin HT. Arsenic: An overview of applications, health, and environmental concerns and removal processes. Critical Reviews in Environmental Science and Technology. 2011;41:435-519. Available:http://dx.doi.org/10.1080/10643380902945771
4. Smedley PL, Knudsen J, Maiga D. Arsenic in groundwater from mineralized Proterozoic basement rocks of Burkina Faso. Applied Geochemistry. 2007; 22:1074–1092. Available:https://doi.org/10.1016/j.apgeochem.2007.01.00
5. Arunima N, Priya C, Brij B, Kapil G, Seema S, Mika S. Removal of emergent pollutants: A review on recent updates and future perspectives on polysaccharide-based composites vis-à-vis traditional

adsorbents. International Journal of Biological Macromolecules. 2024;258:0141-8130.
Available:https://doi.org/10.1016/j.ijbiomac.2023.129092

6. Thomas SYC, Chuah TG, Robiah Y, Gregory FLK, Azni I. Arsenic toxicity, health hazards and removal techniques from water: An overview. Desalination. 2007;217:139-166.
Available:https://doi.org/10.1016/j.desal.2007.01.015
7. McArthur JM, Sikdar PK, Hoque MA, Ghosal U. Waste-water impacts on groundwater: Cl/Br ratios and implications for arsenic pollution of groundwater in the Bengal Basin and Red River Basin, Vietnam. Science of the Total Environment. 2012;437:390 402.
Available:https://doi.org/10.1016/j.scitotenv.2012.07.068
8. Smedley PL, Kinniburgh DG. A review of the source, behaviour and distribution of arsenic in natural.waters. Applied Geochemistry. 2002;17:517-568.
Available:https://doi.org/10.1016/S0883-2927(02)00018-5
9. Ahoulé DG, Lalanne F, Mendret J, Brosillon S, Maïga AH. Arsenic in African Waters: A Review. Water Air Soil Pollution. 2015;226:302.
Available:https://doi.org/10.1007/s11270-015-2558-4
10. Bretzler A, Lalanne F, Nikiema J, Podgorski J, Pfenninger N, Berg M, Schirmer M. Groundwater arsenic contamination in Burkina Faso, West Africa: Predicting and verifying regions at risk. Science of the Total Environment. 2017;84-585:958–970.
Available:https://doi.org/10.1016/j.scitotenv.2017.01.147
11. Nic E, Korte MS, Quintus FPD. A review of arsenic (III) in groundwater. Critical Reviews in Environmental Control. 1991;21:1-39.
Available:http://dx.doi.org/10.1080/10643338910938840
12. Garelick H, Dybowska A, Valsami JE, Priest ND. Remediation technologies for arsenic contaminated drinking waters. Journal of Soils and Sediments. 2005;5:182-190.
Available:https://doi.org/10.1065/jss2005.06.140
13. Yang Y, Ling Y, Kok YK, Chenghong W, Chen JP. Rare-earth metal-based adsorbents for effective removal of arsenic from water: A critical review. Critical Reviews in Environmental Science and Technology. 2018;48:1127-1164.
DOI: 10.1080/10643389.2018.1514930
14. Sadiya A, Shafinaz S, Norahim I, Mohammed JN, Dai VN Vo, Fazilah A Manan. Arsenic removal technologies and future trends: A mini review. Journal of Cleaner Production. 2012;278:0959-6526.
Available:https://doi.org/10.1016/j.jclepro.2020.123805
15. Gupta VK, Saini VK, Neera J. Adsorption of Arsenic (III) from aqueous solutions by iron oxide-coated sand. Journal of Colloid and Interface Science. 2005;288:55– 60.
Available:https://doi.org/10.1016/j.jcis.2005.02.054
16. Mohan DJ, Pittman CU. Arsenic removal from water/wastewater using adsorbents-A critical review. Journal of Hazardous Materials. 2007;142:1–53.
Available:https://doi.org/10.1016/j.jhazmat.2007.01.006
17. Patricia M, Alicia FC. Remediation of arsenic contaminated soils by iron amendments: A review. Critical Reviews in Environmental Science and Technology. 2010;40:93-115.
DOI: 10.1080/10643380802202059
18. Otgon N, Zhang G, Zhang K, Yang C. Removal and fixation of arsenic by forming a complex precipitate containing scorodite and ferrihydrite. Hydrometallurgy. 2019 ;186:58-65.
Available:https://doi.org/10.1016/j.hydromet.2019.03.012
19. Sanou Y. Etude de la performance des charbons actifs, du granulé d'hydroxyde ferrique et de la latérite pour l'élimination de la demande chimique en oxygène, du calcium et de l'arsenic des eaux. Thèse de doctorat unique, Université Ouaga I Pr Joseph KI-ZERBO., Burkina Faso; 2017.
20. Pierce ML, Moore CB. Adsorption of arsenite and arsenate on amorphous iron hydroxide. Water Ressource.1982;16:1247–1253.
Available:https://doi.org/10.1016/0043-1354(82)90143-9
21. Schwertmann U, Cornell RM. Iron oxides in the laboratory: Preparation and characterization weinheim. *Wiley-VCH Verlag Gmb.,* X. 2007;103-112.
Available:https://doi.org/10.1002/9783527613229.ch08

22. Lallan SY, Bijay KM, Arvind K, Kakoli KP. Arsenic removal using bagasse fly ash-iron coated and sponge iron char. Journal of Environmental Chemical Engineering. 2014;3:1467-1473.
Available:https://doi.org/10.1016/j.jece.2014.06.019
23. Saha B, Bains R, Greenwood F. Physicochemical characterization of granular ferric hydroxide (GFH) for arsenic(V) sorption from water. Separation Science and Technology. 2005;40:2909 - 2932.
Available:https://doi.org/10.1080/01496390500333202
24. Yongfeng J, Liying X, Zhen F, George P, Demo P. Observation of surface precipitation of arsenate on ferrihydrite. Environmental Science Technology. 2006;40:3248-3253.
Available:https://doi.org/10.1021/es051872
25. Chen A, Ying L, Jianying S, Yuji A. Ferrihydrite transformation impacted by coprecipitation of phytic acid. Environmental Science and Technology. 2020;14:8837–8847.
Available:https://doi.org/10.1021/acs.est.0c02465
26. Milton VG, Mariana UA, Katherine VE, Mario V, Rodolfo Z, Nadia MV. Laboratory synthesis of goethite and ferrihydrite of controlled particle sizes. Boletín de la Sociedad Geológica Mexicana. 2015;67:433-446.
DOI: 10.18268/BSGM2015v67n3a7
27. Yongfeng J, Liying X, Xin W, George PD. Infrared spectroscopic and X-ray diffraction characterization of the nature of adsorbed arsenate on ferrihydrite. Geochimica et Cosmochimica Acta. 2007;71:1643-1654.
Available:https://doi.org/10.1016/j.gca.2006.12.021.
28. Hélène Laversin. Traceurs et formes chimiques du fer dans les particules émises dans l'atmosphère depuis un site sidérurgique : Etude spectroscopique et caractérisation de composés de référence et de particules collectées dans l'environnement. Thèse unique de Chimie de l'Université du Littoral - Côte d'Opale., République de France; 2006.
29. Parmar C, Parmar GS. Structural and magnetic properties of six-line ferrihydrite nanoparticles. Journal Superconductivity Novel Magnetism. 2020;33:441–444.
Available:https://doi.org/10.1007/s10948-019-05200-x
30. Jia LW, Ming CL, Yen SC, Sook YC, Angnes NTT. The Potential of Fe-Based Magnetic Nanomaterials for the Agriculture Sector. Chemistry Select. 2022;7.
DOI: 10.1002/slct.202104603
31. Qi P, Pichler T. Closer look at As (III) and As (V) adsorption onto ferrihydrite under competitive conditions: Langmuir. Journal American Chemical Society. 2014;30:11110−11116.
Available:https://doi.org/10.1021/la502740w
32. Sanou Y, Nguyen TTP, Paré S, Nguyen VP. Dynamic study and modelling of arsenic removal from groundwater using ferromagnetic carbon as fixed bed adsorbent in column. French-Ukrainian Journal of Chemistry. 2023;11.
DOI: 10.17721/fujcV11I1P74-90
33. Rahman M, Lamb D, Rahman M, Bahar M, Sanderson P. Adsorption-desorption beh avior of arsenate using single and binary iron-modified biochars: Thermodynamics and redox transformation. ACS Omega. 2022;7:101-117.
DOI: 10.1021/acsomega.1c04129
34. Langmuir I. The adsorption of gases on plane surfaces of glass, mica and platinum. Journal of American Chemical Society. 1918;40:1361–1403.
Available:http://dx.doi.org/10.1021/ja02242a004
35. Abinashi S, Jeongwon P, Hyoeun K, Pyung KP. Arsenic removal from aqueous solutions by adsorption onto hydrous Iron oxide-impregnated alginate beads. Journal of Industrial and Engineering Chemistry. 2016;35:277-28.
Available:https://doi.org/10.1016/j.jiec.2016.01.005



*Peer-review history:*
*The peer review history for this paper can be accessed here:*
*https://www.sdiarticle5.com/review-history/114762*